NANO LETTERS
pubs.acs.org/NanoLett

Effect of Spatial Charge Inhomogeneity on 1/*f* Noise Behavior in Graphene

Guangyu Xu,[†] Carlos M. Torres, Jr.,[†] Yuegang Zhang,[*,‡] Fei Liu,[§] Emil B. Song,[†] Minsheng Wang,[†] Yi Zhou,[†] Caifu Zeng,[†] and Kang L. Wang[*,†]

[†] Department of Electrical Engineering, University of California at Los Angeles, Los Angeles, California 90095,
[‡] Molecular Foundry, Lawrence Berkeley National Laboratory, 1 Cyclotron Road, Berkeley, California 94720, and
[§] IBM T. J. Watson Research Center, Yorktown Heights, New York 10598

ABSTRACT Scattering mechanisms in graphene are critical to understanding the limits of signal-to-noise ratios of unsuspended graphene devices. Here we present the four-probe low-frequency noise (1/*f*) characteristics in back-gated single layer graphene (SLG) and bilayer graphene (BLG) samples. Contrary to the expected noise increase with the resistance, the noise for SLG decreases near the Dirac point, possibly due to the effects of the spatial charge inhomogeneity. For BLG, a similar noise reduction near the Dirac point is observed, but with a different gate dependence of its noise behavior. Some possible reasons for the different noise behavior between SLG and BLG are discussed.

KEYWORDS Graphene, spatial charge inhomogeneity, Dirac point, 1/*f* noise

Graphene is a two-dimensional film with intrinsically ultrahigh carrier mobility, showing extraordinary potential for device applications.[1−5] However, most unsuspended graphene sheets are degraded by external perturbations from the environment.[3,6,7] For example, the charged impurity scattering lessens the carrier mobility of substrated graphene devices; the carrier trapping/detrapping near the graphene−substrate interface leads to device variability and contributes to the low frequency (1/*f*) noise.[8,9] Recent work has shown that the random charged impurities near the graphene−substrate interface creates an inhomogeneous charge distribution along the graphene sheet.[10,11] The spatial-charge inhomogeneity in graphene affects the ideal transport properties and is responsible for several physical anomalies near the Dirac point.[12,13] It would be of fundamental interest to investigate how the presence of spatial charge inhomogeneity influences the 1/*f* noise behavior in graphene. A detailed study on the 1/*f* noise behavior of substrated graphene would also help to achieve high-speed carbon-based electronics with high signal-to-noise-ratios.

Multiple groups have conducted research on the 1/*f* noise behavior on graphene nanostructures. Previous work on graphene nanoribbon (with 30 nm width) shows that 1/*f* noise increases as the resistance increases in single layer graphene nanoribbon (SLR), whereas the noise increases as the resistance decreases in bilayer nanoribbon (BLR), which is attributed to the band-gap-opening effect.[8] For bulk graphene (with micrometer width), dual-gated device structures have been used to achieve low noise level in single layer graphene (SLG),[14] and to understand the noise correlation with the band structure in bilayer graphene (BLG).[9] In this work, we present the four-probe low frequency (1/*f*) noise characteristics in SLG and BLG samples using a back-gated device structure. The back-gated structure helps simplify the interface physics in understanding the carrier−substrate interaction.[15,16] We focus on bulk samples with a four-probe setup to reduce the noise contribution from the edge states (as in nanoribbon)[17,18] and the metal contacts,[8,19−21] although the contacts might still affect the electron−hole symmetry in this work.[22,23] For SLG, we find that the noise was reduced either close to or far away from the Dirac point (M-shape); for BLG, we find a similar noise reduction near the Dirac point, but with an increase of the noise away from the Dirac point (V-shape). Our noise data near the Dirac point can be correlated to the spatial-charge inhomogeneity at low carrier density limits; this fact might provide insights to the scattering mechanisms in graphene near the Dirac point.

Graphene sheets were mechanically exfoliated from natural graphite and transferred onto a 300 nm thermally grown SiO_2 dielectric film on highly doped Si substrates. Subsequently, they were identified through optical microscopy and Raman spectroscopy and patterned to form Hall bar and/or multiprobe structures using general e-beam writing processes (inset of Figure 1a).[23,24] The devices are maintained in a vacuum environment to avoid contact oxidation and uncontrollable doping effects from the ambiance.[24] Before the measurements, a 20 min vacuum bakeout (100 °C) process is generally applied to partially desorb contaminants (see Supporting Information).[7] A total of more than 10 out of 40 back-gated devices were studied in our work, and the data shown in this paper come from 4 SLG and 4 BLG samples.

---

[*] To whom correspondence should be addressed, wang@ee.ucla.edu (K.W.) and yzhang5@lbl.gov (Y.Z.).

Received for review: 03/19/2010
Published on Web: 08/04/2010

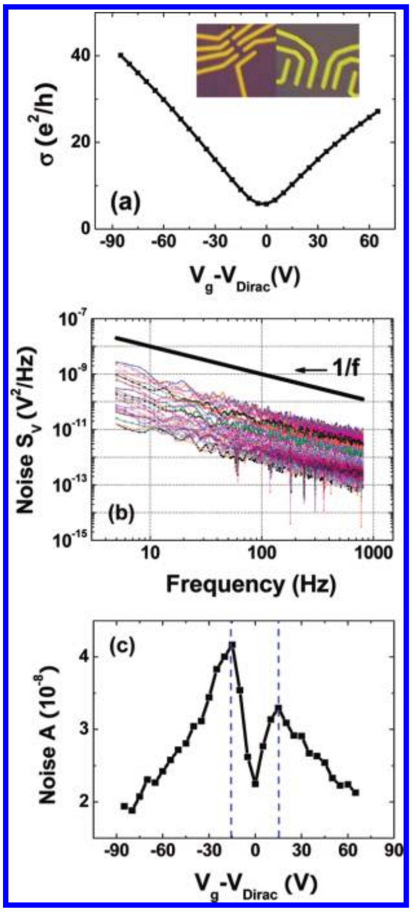

FIGURE 1. Characterization of the bulk single layer graphene (SLG) using dc conductivity and noise measurement. (a) Room temperature dc conductivity versus gate bias ($V_g - V_{Dirac}$) for SLG1. The inset shows the optical pictures of the back-gated Hall bar and multiprobe structures. (b) Room temperature low-frequency noise spectrum of SLG1 with gate biases varying from −50 to 100 V (step = 5 V). The background noise measured at zero current bias has been subtracted from the raw noise data. Four-probe noise spectra (S_V) follow $1/f^\alpha$ behavior with α ranging from 0.85 to 1.12 by biasing V_g both near to and far away from the Dirac point. (c) Noise (A) versus gate bias ($V_g - V_{Dirac}$) for SLG1. An M-shape noise behavior is observed: a noise minimum occurs at the Dirac point, and the two noise maximum points (see the dashed lines) occur on both the electron and hole sides. Neither field-induced nor quantum-confined band gap could contribute to this noise behavior near the Dirac point.[8,26,27]

In the four-probe configuration, an Agilent 4156C was used to apply dc current bias to the device within its linear regime (not shown), and measure its dc conductivity σ; an Agilent 35670A was used to collect the noise spectra of the fluctuations of the potential difference (V) across the graphene samples (see Supporting Information). Figure 1a shows the typical room temperature conductivity versus the gate bias (shifted by V_{Dirac}, the gate bias at Dirac point) for a SLG sample (SLG1). At each gate bias, the conductivity is averaged by 10 times of measurements at the same time of the noise measurement in order to avoid the hysteresis and ensure the consistency of the data.[20] Figure 1b shows the room temperature noise spectra,S_V (after subtracting the background noise,[20,25] see Supporting Informationt), of SLG1 at the same gate biases applied in the conductivity measurement (see Figure 1a). The noise power spectrum density S_V follows a $1/f^\alpha$ behavior with α ranging from 0.85 to 1.12, when biased either close to or away from the Dirac point.

The noise figure $A = fS_V/V^2$ is commonly used to characterize the noise level for current bias conditions.[15] In this work, the noise is normalized as

$$A = \frac{1}{Z}\sum_{i=1}^{Z} f_i S_{Vi}/V^2$$

which takes the average over the frequency ranges where the noise spectra follow with $1/f^\alpha$ behavior (α ranging from 0.85 to 1.12). This definition helps reduce the measurement errors of the noise at specific frequencies[8,20] and rule out other types of noise sources (e.g., thermal noise, ac electricity power noise, etc).[9,25] For SLG1, the gate dependence of the normalized noise, A, shows an M-shape behavior (see Figure 1c). The noise curve shows a local minimum at the Dirac point and two local maxima near the Dirac point at both the electron- ($V_g-V_{Dirac} > 0$) and hole-conduction ($V_g-V_{Dirac} < 0$) sides. The noise reduction observed in SLG near the Dirac point is different from most electronic materials (including SLR), where the noise increases with sample resistance.[8]

We measured SLG samples under different conditions to rule out extrinsic possibilities for the M-shape noise behavior. First, this M-shape noise behavior was found to be independent of the types of the initial doping ($V_{Dirac\text{-}SLG1} > 0$, $V_{Dirac\text{-}SLG2} \sim 0$, $V_{Dirac\text{-}SLG3} < 0$, see Figure 2a). Second, the measurements have been repeated by sweeping the gate voltage back and forth (not shown), to ensure that the noise behavior is independent of the mobile ions close to the graphene$-$SiO$_2$ interface.[26] Third, the noise level was independent of the current biases (see Supporting Information), showing that the noise of graphene is from the resistance fluctuations[19,27,28] and not affected by the current-induced local heating effects.[24,29] Overall, the M-shape noise behavior is universal in our measurements and suggests to originate from the intrinsic trapping/detrapping processes near the graphene$-$SiO$_2$ substrate in SLG.

To gain some insights of the M-shape noise behavior, it helps to see where the noise starts to reduce near the Dirac point. The spatial average carrier density could be defined as $\langle n\rangle = C_g(V_g - V_{Dirac})/e$,[24,26] when $\langle n\rangle$ is not less than the density of charged impurities n_{imp}.[30] Figure 2b shows that the noise maximum generally occurs at$|\langle n_{noisemax}\rangle| = 1-1.6 \times 10^{12}$ cm^{-2}, a value approximately equal to the estimated $n_{imp} = 1-2 \times 10^{12}$ cm^{-2} in our SLG samples[31,32] (Note: the charged impurity density, n_{imp}, used in this work is estimated as the theoretical $\sigma_{Dirac} - n_{imp}$ and $\mu - n_{imp}$ relations based on the self-consistent approximation; see refs 31 and32). It is accepted that the transport properties of SLG near the Dirac point (i.e., $|\langle n\rangle| < n_{imp}$) are dominated by the spatial charge inhomogeneity, when the landscape of SLG is broken into puddles of electrons and holes.[30,33] Our data show that the noise of SLG starts to reduce when $|\langle n\rangle| < n_{imp}$, which

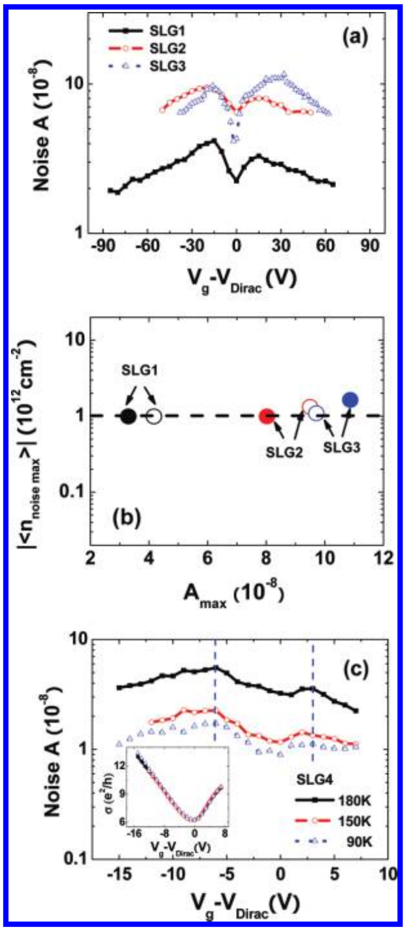

FIGURE 2. Noise data of single layer graphene (SLG). (a) Room temperature noise (A) versus gate bias ($V_g - V_{\text{Dirac}}$) for SLG1, SLG2, and SLG3. All SLG samples show an M-shape noise behavior, which is independent of the types of the initial doping ($V_{\text{Dirac-SLG1}} > 0$, $V_{\text{Dirac-SLG2}} \sim 0$, $V_{\text{Dirac-SLG3}} < 0$). The noise behavior is repeatable by changing the direction of the injection current through the samples. (b) Spatial average carrier density of the noise maximum ($|\langle n_{\text{noisemax}}\rangle|$) versus the value of noise maximum (A_{max}), for both the electron-conduction (solid circles, $V_g - V_{\text{Dirac}} > 0$) and hole-conduction (hollow circles, $V_g - V_{\text{Dirac}} < 0$) sides. The noise maximum points at both sides are shown at $|\langle n_{\text{noisemax}}\rangle| = 1-1.6 \times 10^{12}$ cm^{-2}. It is estimated that $n_{\text{imp}} = 1-2 \times 10^{12}$ cm^{-2} ($r_s = 0.8$, $d = 1$ nm) in our SLG samples using the theoretical methods.[31,32] (c) Temperature dependence of the noise behavior for SLG4. The M-shape noise behavior does not change with the temperature down to 90 K. The noise level is shown to monotonously decrease with the temperature. The inset shows the weak temperature dependence of dc conductivity versus the gate bias ($V_g - V_{\text{Dirac}}$) for SLG4. The dashed vertical lines show that the noise maximum is independent of the temperature.

suggests that the noise behavior near the Dirac point correlates with the spatial charge inhomogeneity. The value of the noise maximum, A_{max}, is almost equal for both the electron- and hole-conduction sides (10^{-8}–10^{-7}), while some differences might be from the electron–hole asymmetry induced by the doping effect of metal contacts.[23]

Up to now, a noise model of graphene materials considering the spatial charge inhomogeneity is still lacking.[8,9] Admitting the complexity of this problem, here we try to use a qualitative approach to give some phenomenological explanations. Some assumptions are made to simplify the discussion:

(1) Close to the Dirac point, electrons and holes transport along the puddles of electrons and holes, respectively;[26,30] hence both types of carriers would contribute to the noise. By neglecting the electron–hole interaction, we assume these two types of carriers independently interact with the active traps (see Supporting Information) in their puddle regions, respectively.

(2) Previous work shows that two types of puddle regions exist in SLG near the Dirac point:[26,32,33] (I) wide regions (over the whole graphene sheet) with almost uniform low carrier densities;[26,32] (II) narrow regions (typical size ~10 nm) with much higher carrier densities. We neglect the contribution of the noise from type II regions since they are highly conductive (better screening to active traps) and only occupy a small portion (<20%).[32,33] Hence, the noise mainly comes from the type I regions, where the carrier density is almost uniform ($n_{\text{electron}}^{\text{TypeI}} \sim$ constant, $n_{\text{hole}}^{\text{TypeI}} \sim$ constant).

(3) Hooge's empirical equation $A = fS_V/V^2 = \alpha_H/N$ is well-defined for homogeneous materials;[27,34] this equation generally needs to be modified for inhomogeneous materials by weighting each local area differently.[21,27] On the basis of (1) and (2), however, we see the total noise mainly comes from two independent type I regions for both electrons and holes, respectively. Since type I regions are nearly homogeneous, the total noise could be estimated as

$$A = A_{\text{electron}} + A_{\text{hole}} \sim \frac{\alpha_H}{N_{\text{electron}}^{\text{TypeI}}} + \frac{\alpha_H}{N_{\text{hole}}^{\text{TypeI}}} \sim \frac{\alpha_H}{n_{\text{electron}}^{\text{TypeI}} D_{\text{electron}}^{\text{TypeI}}} + \frac{\alpha_H}{n_{\text{hole}}^{\text{TypeI}} D_{\text{hole}}^{\text{TypeI}}}$$

($A_{\text{electron(hole)}}$ is the noise from electrons (holes); $N_{\text{electron(hole)}}^{\text{TypeI}}$ and $D_{\text{electron(hole)}}^{\text{TypeI}}$ are the total number of electrons (holes) and the area of type I regions for electrons (holes), respectively).[8,9,14] The electron–electron (hole–hole) interaction is neglected, because Hooge's law implies that each carrier is considered to interact with active traps independently.[27,34]

In the following, we limit the discussion to the noise behavior at the Dirac point and the electron conduction side ($V_g - V_{\text{Dirac}} > 0$), since the hole conduction side ($V_g - V_{\text{Dirac}} < 0$) could be explained similarly.

(1) The Noise at the Dirac Point. At the Dirac point, charge neutrality is satisfied ($N_{\text{electron}}^{\text{TypeI}} \sim N_{\text{hole}}^{\text{TypeI}}$). Due to the existence of the spatial charge inhomogeneity, the total noise is given as

$$A \sim \frac{2\alpha_H}{N_{\text{electron}}^{\text{TypeI}}} \sim \frac{2\alpha_H}{n_{\text{rms}} D_{\text{electron}}^{\text{TypeI}}}$$

(here we define n_{rms} as the root mean square of spatial density fluctuations at the Dirac point, and $|n_{\text{electron}}^{\text{TypeI}}| \sim |n_{\text{hole}}^{\text{TypeI}}| \sim n_{\text{rms}}$ at the Dirac point[32,33]). Thus, the noise at the Dirac point is determined from the carrier density fluctuations caused by spatial charge inhomogeneity in SLG.

(2) Noise Behavior before the Noise Maximum. Between the Dirac point and the noise maximum, one type of carrier (i.e., majority) would dominate the other (i.e., minority). As the gate bias increases ($V_g - V_{\mathrm{Dirac}} > 0$): (a) $n_{\mathrm{electron(hole)}}^{\mathrm{TypeI}}$ increases (decreases) (i.e., $n_{\mathrm{hole}}^{\mathrm{TypeI}} < n_{\mathrm{electron}}^{\mathrm{TypeI}}$), and $n_{\mathrm{electron(hole)}}^{\mathrm{TypeI}} \propto V_g - V_{\mathrm{Dirac}}$[24,26] (type-I regions are nearly homogeneous). Thus, $\Delta(n_{\mathrm{hole}}^{\mathrm{TypeI}}) \sim \Delta(n_{\mathrm{electron}}^{\mathrm{TypeI}})$. (b) $D_{\mathrm{electron(hole)}}^{\mathrm{TypeI}}$ increases (decreases) (i.e., $D_{\mathrm{hole}}^{\mathrm{TypeI}} < D_{\mathrm{electron}}^{\mathrm{TypeI}}$), and $\Delta(D_{\mathrm{hole}}^{\mathrm{TypeI}}) \sim \Delta(D_{\mathrm{electron}}^{\mathrm{TypeI}})$. (c) The noise

$$A_{\mathrm{electron(hole)}} \sim \frac{\alpha_{\mathrm{H}}}{N_{\mathrm{electron(hole)}}^{\mathrm{TypeI}}} \sim \frac{\alpha_{\mathrm{H}}}{n_{\mathrm{electron(hole)}}^{\mathrm{TypeI}} D_{\mathrm{electron(hole)}}^{\mathrm{TypeI}}}$$

decreases (increases). Thus, $A_{\mathrm{hole}} > A_{\mathrm{electron}}$. The overall effect is

$$\begin{aligned}\Delta(A_{\mathrm{hole}}) &\sim A_{\mathrm{hole}}\left[\frac{\Delta(n_{\mathrm{hole}}^{\mathrm{TypeI}})}{n_{\mathrm{hole}}^{\mathrm{TypeI}}} + \frac{\Delta(D_{\mathrm{hole}}^{\mathrm{TypeI}})}{D_{\mathrm{hole}}^{\mathrm{TypeI}}}\right]\\ &> A_{\mathrm{electron}}\left[\frac{\Delta(n_{\mathrm{electron}}^{\mathrm{TypeI}})}{n_{\mathrm{electron}}^{\mathrm{TypeI}}} + \frac{\Delta(D_{\mathrm{electron}}^{\mathrm{TypeI}})}{D_{\mathrm{electron}}^{\mathrm{TypeI}}}\right] \sim \Delta(A_{\mathrm{electron}})\end{aligned}$$

an increase of noise from holes greater than a decrease of noise from electrons. Therefore, the total noise increases ($\Delta A = \Delta(A_{\mathrm{hole}}) - \Delta(A_{\mathrm{electron}}) > 0$) as we move away from the Dirac point before reaching the noise maximum.

(3) Noise Behavior beyond the Noise Maximum. As the gate bias keeps increasing, $D_{\mathrm{hole}}^{\mathrm{TypeI}}$ continues shrinking and the hole-puddle region becomes sparse and cannot form a path for hole conduction.[26,32,33] When those isolated hole islands stop contributing to the noise (even though they have small $n_{\mathrm{hole}}^{\mathrm{TypeI}}$ and $D_{\mathrm{hole}}^{\mathrm{TypeI}}$), the total noise only comes from the electrons as

$$A \sim A_{\mathrm{electron}} \sim \frac{\alpha_{\mathrm{H}}}{N_{\mathrm{electron}}^{\mathrm{TypeI}}}$$

Hence, the total noise will decrease as the gate bias further increases, because more electrons effectively screen the active traps.

On the basis of (2) and (3), we suggest the noise maximum point occurs when the holes (minority) stop dominating the noise behavior (become isolated and not conducting). Under this physical picture, we estimate the noise maximum point as follows: at the Dirac point $|n_{\mathrm{hole}}^{\mathrm{TypeI}}| \sim n_{\mathrm{rms}}$, whereas at the noise maximum $|n_{\mathrm{hole}}^{\mathrm{TypeI}}|$ becomes negligible. In order to modulate $|n_{\mathrm{hole}}^{\mathrm{TypeI}}|$ from n_{rms} to near zero, a gate bias that is equivalent to the spatial average density $\sim n_{\mathrm{rms}}$ is required ($n_{\mathrm{hole}}^{\mathrm{TypeI}} \propto V_g - V_{\mathrm{Dirac}}$). Thus, the noise maximum occurs near $|\langle n_{\mathrm{noisemax}}\rangle| \sim n_{\mathrm{rms}}$. This estimate is consistent with the experimental data in Figure 2b ($|\langle n_{\mathrm{noisemax}}\rangle| \sim n_{\mathrm{imp}}$), since theoretical works show that $n_{\mathrm{rms}} \sim n_{\mathrm{imp}}$ for typical $n_{\mathrm{imp}} \sim 10^{11}-10^{12}$ cm^{-2}.[31,32]

To further understand the noise mechanism, we measured another SLG sample (SLG4) under temperatures from 180 to 90 K (see Figure 2c), where the noise spectra all follow the $1/f$ behavior. The noise at all gate biases decreases when temperature decreases, possibly because some active traps become frozen (kT) and stop contributing to the noise.[27,28] The weak temperature dependence of the dc conductivity (see inset) confirms that the transport is limited by charged impurity scattering.[24,33] Similarly, the M-shape noise behavior is shown for all temperatures, and the noise maximum points (for both the electron- and hole-conduction sides) do not change with temperature. The data suggest that the distribution of spatial charge inhomogeneity is almost unchanged (n_{imp},n_{rms}) with the temperature as predicted.[31,32] It is noted that the region of the noise reduction near the Dirac point (the dip in M-shape) is narrower (smaller $|\langle n_{\mathrm{noisemax}}\rangle|$) than those in SLG1−SLG3. This can be attributed to a smaller spatial charge inhomogeneity in SLG4. ($n_{\mathrm{imp}}/n_{\mathrm{rms}} \sim 7 \times 10^{11}$ cm^{-2}, estimated carrier mobility (ref 24) μ_e, $\mu_h \sim 4000$ cm^2/(V · s) whereas μ_e, $\mu_h < 3000$ cm^2/(V · s) for SLG1−SLG3).

So far, we attributed the M-shape noise behavior of SLG to the spatial charge inhomogeneity. For our SLG samples, the M-shape noise behavior is consistently observed. However, we do not deny that some high-quality SLG samples (n_{imp}, $n_{\mathrm{rms}} \rightarrow 0$) might not show the noise reduction near the Dirac point ($|\langle n_{\mathrm{noisemax}}\rangle| \rightarrow 0$). The fact that our noise spectra do not deviate from $1/f$ behavior at low temperature suggests the existence of multiple active traps ($\gg 1$) in our SLGs,[19,21] where the Hooge parameter α_{H} is estimated to be $10^{-3}-10^{-2}$ away from V_{Dirac} for both electron- and hole-conduction sides. Moreover, detailed noise modeling considering the carrier−carrier interactions (e−e, h−h, e−h interactions) and the noise contribution from the small type II regions is needed to further understand the noise behavior quantitatively.

We also examine the noise behavior of BLG samples. Three back-gated BLG samples are measured ($V_{\mathrm{Dirac\text{-}BLG3}} < V_{\mathrm{Dirac\text{-}BLG1}} < V_{\mathrm{Dirac\text{-}BLG2}} < 0$) at room temperature; they all exhibit a V-shape noise behavior (see Figure 3a), showing a similar noise reduction near the Dirac point to that of SLG. Temperature-dependent measurement (BLG4, from 300 to 77 K) exhibits results qualitatively similar to SLG (see Figure 3b): the transport shows weak temperature dependence; the V-shape noise behavior is observed for all temperatures, where the $1/f$ noise spectra remain and α_{H} ranges in the same order of those in SLGs.

A recent work observed the V-shape noise behavior in dual-gated BLG samples as well,[9] which has been attributed to the band-gap-opening in the BLG band structure. While this might be the reason, the gate-induced band gap in back-gated BLG still lacks experimental evidence from electrical transport measurement[35,36]

Admitting that the effect of the band-gap opening on the noise behavior of BLG may be possible, here we try to consider another scenario. In a gapless situation, the transport of BLG near Dirac point has been suggested to resemble that of SLG where the spatial charge inhomogeneity breaks the density landscape into puddles of electrons and holes.[37,38]

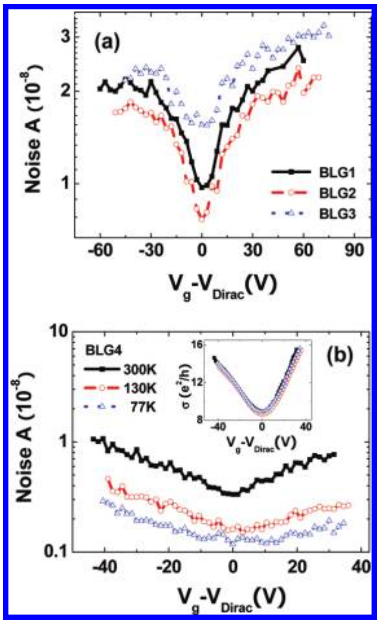

FIGURE 3. Noise data of bilayer graphene (BLG). (a) Room temperature noise (A) vs gate bias ($V_g - V_{\mathrm{Dirac}}$) for BLG1, BLG2, and BLG3. All BLG samples show a V-shape noise behavior ($V_{\mathrm{Dirac\text{-}BLG3}} < V_{\mathrm{Dirac\text{-}BLG1}} < V_{\mathrm{Dirac\text{-}BLG2}} < 0$). The noise measurements have been repeated to rule out the effects from mobile ions and local heating. The V-shape noise behavior is shown to be universal in our BLG samples. (b) Temperature dependence of the noise behavior for BLG4. The V-shape noise behavior does not change with the temperature from 300 to 77 K. Similar to SLG, the noise level is shown to monotonously decrease with the temperature, possibly because some active traps are frozen. The inset shows the weak temperature dependence of dc conductivity versus the gate bias ($V_g - V_{\mathrm{Dirac}}$) for BLG4.

Indeed, a recent STM experiment shows the existence of spatial charge inhomogeneity in back-gated BLG at the Dirac point.[39] Hence, we propose that the noise behavior of BLG near the Dirac point could also be correlated with the spatial charge inhomogeneity: At the Dirac point, the noise is determined by $|n_{\mathrm{electron}}^{\mathrm{TypeI}}| \sim |n_{\mathrm{hole}}^{\mathrm{TypeI}}| \sim n_{\mathrm{rms}}$, and away from Dirac point, the noise increases possibly because of the noise increase from the minority carriers (e.g., holes for $V_g - V_{\mathrm{Dirac}} > 0$), $\Delta A = \Delta(A_{\mathrm{minority}}) - \Delta(A_{\mathrm{majority}}) > 0$. The noise in BLG, however, does not decrease at higher biases as the case in SLG, showing a V-shape instead of an M-shape. The reason may come from the large spatial charge inhomogeneity (even in clean samples) of BLG: due to their different dispersion relationships, BLG has been predicted to have a larger n_{rms} than that in SLG under the same disorder level (n_{imp}).[37,38] Hence, BLG would qualitatively have a wider gate range where the noise is contributed from both electrons and holes and increases with the gate bias (refer to the noise behavior between the Dirac point and the noise maximum in SLG). Overall, the V-shape noise behavior of BLG could be from the band-gap-opening effect and/or spatial charge inhomogeneity.

In conclusion, we present the low-frequency noise behavior in back-gated SLG (M-shape) and BLG (V-shape) samples, both with weak temperature dependence (down to 77K). Using a qualitative approach, the noise behavior near the Dirac point suggests relevance to the spatial charge inhomogeneity in SLG and BLG samples. A quantitative noise model of graphene is necessary to deepen the understanding. Fundamentally, low-frequency noise describes the trapping/detrapping processes near the graphene$-$SiO$_2$ interface, while more efforts are needed to gain further insights on the scattering mechanisms of graphene. Moreover, this work may help predict, control, and improve the signal-to-noise ratio of substrated graphene devices and suppress the phase distortion for high-frequency applications.

Acknowledgment. The authors gratefully acknowledge the discussions from F. Miao, X. Zhang, and F. X. Xiu, and experimental help from S. Aloni, T. Kuykendall, Z. J. Xu, and J. W. Bai. We thank E. Rossi, E. H. Hwang, and S. Adam from S. Das Sarma's group for theoretical discussions. This work was in part supported by MARCO Focus Center on Functional Engineered Nano Architectonics (FENA), monitored by Dr. Betsy Weitzman. The work at the Molecular Foundry was supported by the Office of Science, Office of Basic Energy Sciences, of the U.S. Department of Energy under Contract No. DE-AC02-05CH11231.

Supporting Information Available. Description of device preparation and noise measurement, definition of the noise figure, and discussion of the active traps and its relation with charged impurities, table of sheet dimensions of graphene samples, and figures of Raman spectroscopy and images of graphene sheets, scheme of four-probe configuration of 1/f noise measurement, and noise independence on current biases. This material is available free of charge via the Internet at http://pubs.acs.org.

REFERENCES AND NOTES

(1) Novoselov, K. S.; et al. Electric field effect in atomically thin carbon films. *Science* **2004**, *306*, 666–669.
(2) Morozov, S. V.; et al. Giant intrinsic carrier mobilities in graphene and its bilayer. *Phys. Rev. Lett.* **2008**, *100*, No. 016602.
(3) Du, X.; et al. Approaching ballistic transport in suspended graphene. *Nat. Nanotechnol.* **2008**, *3*, 491–495.
(4) Hong, X.; et al. High-mobility few-layer graphene field effect transistors fabricated on epitaxial ferroelectric gate oxide. *Phys. Rev. Lett.* **2009**, *102*, 136808.
(5) Lin, Y. M.; et al. Operation of graphene transistors at gigahertz frequencies. *Nano Lett.* **2009**, *9*, 422–426.
(6) Chen, J. H.; et al. Intrinsic and extrinsic performance limits of graphene devices on SiO$_2$. *Nat. Nanotechnol.* **2008**, *3*, 206–209.
(7) Chen, J. H.; et al. Charged-impurity scattering in graphene. *Nat. Phys.* **2008**, *4*, 377–381.
(8) Lin, Y. M.; Avouris, P. Strong suppression of electrical noise in bilayer graphene nanodevices. *Nano Lett.* **2008**, *8*, 2119–2125.
(9) Pal, A. N.; Ghosh, A. Resistance noise in electrically biased bilayer graphene. *Phys. Rev. Lett.* **2009**, *102*, 126805.
(10) Martin, J.; et al. Observation of electron-hole puddles in graphene using a scanning single-electron transistor. *Nat. Phys* **2008**, *4*, 144–148.
(11) Zhang, Y. B.; et al. Origin of spatial charge inhomogeneity in graphene. *Nat. Phys.* **2009**, *5*, 722–726.
(12) Heersche, H. B.; et al. Bipolar supercurrent in graphene. *Nature* **2007**, *446*, 56–59.
(13) Wei, P.; et al. Anomalous thermoelectric transport of Dirac particles in graphene. *Phys. Rev. Lett.* **2009**, *102*, 166808.
(14) Gang, L.; et al. Low-frequency electronic noise in the double-gate single-layer graphene transistors. *Appl. Phys. Lett.* **2009**, *95*, No. 033103.

(15) Lin, Y. M.; et al. Low-frequency current fluctuations in individual semiconducting single-wall carbon nanotube. *Nano Lett.* **2006**, *6*, 930–936.

(16) Jang, C.; et al. Tuning the effective fine structure constant in graphene: Opposing effects of dielectric screening on short- and long-range potential scattering. *Phys. Rev. Lett.* **2008**, *101*, 146805.

(17) Evaldsson, M. Edge-disorder-induced Anderson localization and conduction gap in graphene nanoribbons. *Phys. Rev. B* **2008)** , *78*, 161407 (R).

(18) Barone, V.; et al. Electronic structure and stability of semiconducting graphene nanoribbons. *Nano Lett.* **2006**, *6*, 2748–2754.

(19) Tobias, D. Origins of 1/f noise in individual semiconducting carbon nanotube field-effect transistors. *Phys. Rev. B* **2008**, *77*, No. 033407.

(20) Xu, G.; et al. Low-frequency noise in top-gated ambipolar carbon nanotube field effect transistors. *Appl. Phys. Lett.* **2008**, *92*, 223114.

(21) Kolek, A.; et al. Low-frequency 1/f noise of RuO_2-glass thick resistive films. *J. Appl. Phys.* **2007**, *102*, 103718.

(22) Lee, E. J. H.; et al. Contact and edge effects in graphene devices. *Nat. Nanotechnol.* **2008**, *3*, 486–490.

(23) Han, W. Electron-hole asymmetry of spin injection and transport in single-layer graphene. *Phys. Rev. Lett.* **2009**, *102*, 137205.

(24) Tan, Y. W.; et al. Measurement of scattering rate and minimum conductivity in graphene. *Phys. Rev. Lett.* **2007**, *99*, 246803.

(25) Snow, E. S.; et al. 1/f noise in single-walled carbon nanotube devices. *Appl. Phys. Lett.* **2004**, *85*, 4172–4174.

(26) Rossi, E.; Sarma, S. D. Ground state of graphene in the presence of random charged impurities. *Phys. Rev. Lett.* **2008**, *101*, 166803.

(27) Van Der Zeil, A. Unified presentation of l/f noise in electronic devices: fundamental l/f noise sources. *Proc. IEEE* **1988**, *76* (No. 3), 233–258.

(28) Huang, K. K.; et al. A unified model for the flicker noise in metal-oxide-semiconductor field-effect transistors. *IEEE Trans. Electron Devices* **1990**, *37*, 654–665.

(29) Barreiro, A.; et al. Transport properties of graphene in the high-current limit. *Phys. Rev. Lett.* **2009**, *103*, No. 076601.

(30) Hwang, E. H.; et al. Carrier transport in two-dimensional graphene layers. *Phys. Rev. Lett.* **2007**, *98*, 186806.

(31) Adam, S.; et al. A self-consistent theory for graphene transport. *Proc. Natl. Acad. Sci. U.S.A.* **2007**, *104*, 18392–18397.

(32) Rossi, E.; et al. Effective medium theory for disordered two-dimensional graphene. *Phys. Rev. B* **2009**, *79*, 245423.

(33) Adam, S.; et al. Theory of charged impurity scattering in two-dimensional graphene. *Solid State Commun.* **2009**, *149*, 1072–1079.

(34) Hooge, F. N. l/f noise sources. *IEEE Trans. Electron Devices* **1994**, *41*, 1926–1935.

(35) Zhang, Y. B.; et al. Direct observation of a widely tunable bandgap in bilayer graphene. *Nature* **2009**, *459*, 820–823.

(36) Oostinga, J. B.; et al. Gate-induced insulating state in bilayer graphene devices. *Nat. Mater.* **2008**, *7*, 151–157.

(37) Adam, S.; Sarma, S. D. Boltzmann transport and residual conductivity in bilayer graphene. *Phys. Rev. B* **2008**, *77*, 115436.

(38) Sarma, S. D.; Hwang, E. H.; Rossi, E. Theory of carrier transport in bilayer graphene. *Phys. Rev. B* **2010**, *81*, 161407(R). (See link at: http://prb.aps.org/abstract/PRB/v81/i16/e161407).

(39) Danshpande, A.; et al. Mapping the Dirac point in gated bilayer graphene. *Appl. Phys. Lett.* **2009**, *95*, 243502.